Magnetic structure and orbital state of $Ca_3Ru_2O_7$ investigated by resonant x-ray diffraction

B. Bohnenbuck,[1] I. Zegkinoglou,[1] J. Strempfer,[2] C. Schüßler-Langeheine,[3] C. S. Nelson,[4] Ph. Leininger,[1] H.-H. Wu,[3] E. Schierle,[5] J. C. Lang,[6] G. Srajer,[6] S. I. Ikeda,[7] Y. Yoshida,[7] K. Iwata,[8] S. Katano,[8] N. Kikugawa,[9] and B. Keimer[1]

[1]*Max -Planck -Institut für Festkörperforschung, Heisenbergstr. 1, 70569 Stuttgart, Germany*

[2]*Hamburger Synchrotronstrahlungslabor (HASYLAB) at DESY, Notkestr. 85, 22603 Hamburg, Germany*

[3]*II. Physikalisches Institut, Universität zu Köln, Zülpicher Straße 77, 50937 Köln, Germany*

[4]*National Synchrotron Light Source, Brookhaven National Laboratory, Upton, New York 11973-5000, USA*

[5]*Hahn-Meitner-Institut (HMI) at BESSY, Albert Einstein Straße 15, 12489 Berlin, Germany*

[6]*Advanced Photon Source, Argonne National Laboratory, Argonne, Illinois 60439, USA*

[7]*National Institute of Advanced Industrial Science and Technology, Tsukuba, Ibaraki 305-8568, Japan*

[8]*Faculty of Science, Saitama University, Saitama 338-8570, Japan*

[9]*National Institute for Material Science, Tsukuba, Ibaraki 305-0047, Japan*

(Received 14 March 2008; published 5 June 2008)

Resonant x-ray diffraction at the L_2- and L_3-absorption edges of Ru has been used to investigate the magnetic structure of $Ca_3Ru_2O_7$, a material with a bilayer perovskite structure that undergoes a transition from a high-temperature metallic to a low-temperature insulating phase at 48 K. In the insulating phase, magnetic Bragg reflections characteristic of *A*-type antiferromagnetic order (that is, ferromagnetic RuO_2 bilayers coupled antiferromagnetically along the *c*-axis) were identified. The azimuthal-angle dependence of the diffracted intensity implies that the magnetic moments are aligned along the *b*-axis in the RuO_2 planes. In the metallic phase, the *A*-type magnetic order persists up to the Néel temperature of 56 K, but the sublattice magnetization decreases by a factor of ~1.7 and rotates by 90° within the planes. Resonant signals characteristic of uniform or staggered orbital order were not found within the experimental sensitivity, probably reflecting a weak orbital polarization in the insulating state.

DOI: 10.1103/PhysRevB.77.224412 PACS number(s): 78.70.Ck, 75.50.Ee

I. INTRODUCTION

Layered perovskite ruthenates exhibit a wide variety of interesting physical phenomena due to the interplay of spin, charge, lattice, and orbital degrees of freedom. Prominent examples include the *p*-wave superconducting state[1] in Sr_2RuO_4, whose unit cell encompasses one RuO_2 layer, and the electronic liquid-crystal state[2] recently discovered at high magnetic fields in $Sr_3Ru_2O_7$, which exhibits a bilayer perovskite structure. The Ca analogs of these two materials, Ca_2RuO_4 and $Ca_3Ru_2O_7$, have lower electrical conductivities and undergo first-order transitions between high-temperature metallic and low-temperature insulating phases at 357 and 48 K, respectively. The phase diagram of $Ca_3Ru_2O_7$ is particularly interesting as multiple phase transitions are induced by external magnetic fields,[3–5] uniaxial or hydrostatic pressure,[6–8] and doping.[9,10] Most of these transitions have been attributed to rearrangements of the magnetic and/or orbital ordering pattern. As recently demonstrated for Ca_2RuO_4, resonant x-ray diffraction (RXD) is a highly sensitive probe of magnetic and orbital ordering phenomena in the ruthenates. Specifically, a uniform polarization of the Ru 4*d* valence orbitals was observed in the insulating phase of Ca_2RuO_4[11] and a separate phase transition associated with the onset of a staggered component of the orbital ordering pattern was reported at lower temperatures.[12] Here, we report the results of a study in which the methods developed in Refs. 11 and 12 were applied to $Ca_3Ru_2O_7$.

$Ca_3Ru_2O_7$ has an orthorhombic crystal structure described by the space group $Bb2_1m$ with lattice parameters $a=5.3677$, $b=5.5356$, and $c=19.5219$ Å at 8 K.[13] Upon cooling from room temperature, the resistivity exhibits a metallic temperature dependence. At $T_N=56$ K, the material orders antiferromagnetically, but initially remains metallic. At $T_{MI}=48$ K, the resistivity along the *c*-axis abruptly increases and continues to increase upon further cooling.[14,15] Although the resistivity in the *ab*-plane is less strongly affected by the transition and only weakly temperature dependent below T_{MI},[16] we refer to this transition as a metal-insulator transition. This transition is accompanied by large structural modifications including a contraction along the *c*-axis[17] and an in-plane expansion.[13] Below T_{MI}, the existence of orbital order[18] and the formation of a density wave[19,20] have been proposed based on the results of spectroscopic experiments. Magnetometry,[3] Raman scattering,[8] and powder neutron diffraction[13] data suggest an *A*-type antiferromagnetic (AFM) structure (that is, antiferromagnetically stacked ferromagnetic RuO_2 layers) with a magnetic moment direction along the *b*-axis in the low-temperature phase. However, as only a single magnetic Bragg reflection was detected in the neutron diffraction pattern,[13] the magnetic structure assignment must be regarded as tentative. Furthermore, a spin reorientation in the *ab*-plane has been reported at T_{MI}.[3,6,16]

We have investigated the magnetic structure of $Ca_3Ru_2O_7$ using polarized RXD at the *L*-absorption edges of Ru. Two magnetic Bragg reflections were detected and the azimuthal-angle dependence of the Bragg intensities fully confirms the previously suggested *A*-type AFM structure with a *b*-axis moment orientation below T_{MI}. In the magnetically ordered metallic state between T_{MI} and T_N, the *A*-type order persists, but the amplitude of the sublattice magnetization inferred from our data decreases by a factor of ~1.7 and its direction rotates by 90° with respect to the insulating phase. Superlat-

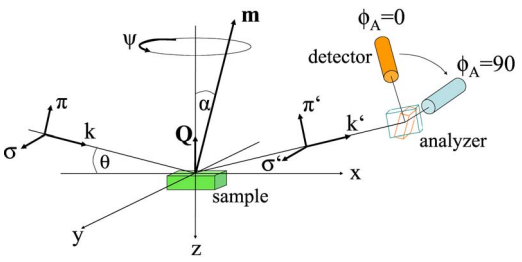

FIG. 1. (Color online) Schematic picture of the experimental setup.

tice reflections characteristic of staggered orbital order were not found and an experiment designed to check for a possible uniform orbital polarization in the low-temperature phase did not yield any signal outside the experimental sensitivity limit. The results are discussed in comparison to the corresponding data on Ca_2RuO_4.

II. EXPERIMENTAL DETAILS

The single crystalline samples were grown at the University of St. Andrews and at the National Institute of Advanced Industrial Science using the floating zone method. Details of the growth technique and the sample characterization have been given elsewhere.[16] The crystals are platelet shaped with the *c*-axis along the short axis and typical dimensions $2\times1\times0.2$ mm^3. They are almost untwinned, that is, the population ratio of the orthorhombic twin domains is smaller than 0.1. The rocking curves have full widths at half maximum of less than 0.15°.

Experiments at the Ru *L*-absorption edges were carried out at beam line 4ID-D of the Advanced Photon Source at Argonne National Laboratory and at beam line KMC1 of the Berliner Elektronenspeicherring Gesellschaft für Synchrotronstrahlung (BESSY). A sketch of the experimental setup is shown in Fig. 1. At 4ID-D, the sample was mounted in a closed-cycle cryostat capable of reaching temperatures between 10 and 350 K, which was mounted on an eight-circle diffractometer with vertical scattering geometry. To minimize absorption effects, the flight path was either kept under vacuum or in He atmosphere and the number of Be windows in the beam path was minimized. The scattered intensity was detected by a NaI scintillation detector, which was combined with a Si (111) crystal for the polarization analysis. At KMC1, a UHV two-circle diffractometer designed by the Freie Universität Berlin was used in horizontal scattering geometry. The sample was mounted on a copper goniometer head which was attached to the cryostat, allowing a manual rotation of the sample about the scattering vector. Sample temperatures as low as 17 K were reached with this setup. The magnetic signal was detected using a silicon-diode photon detector together with a Si (111) crystal as polarization analyzer. The experiment at the *K*-absorption edge of Ru was performed at the 7T-MPW-MagS beam line at BESSY. There, the sample was mounted in a closed cycle cryostat on a eight-circle diffractometer with a vertical scattering plane. The polarization analysis was carried out with the (0,0,16) reflection of a pyrolytic graphite crystal.

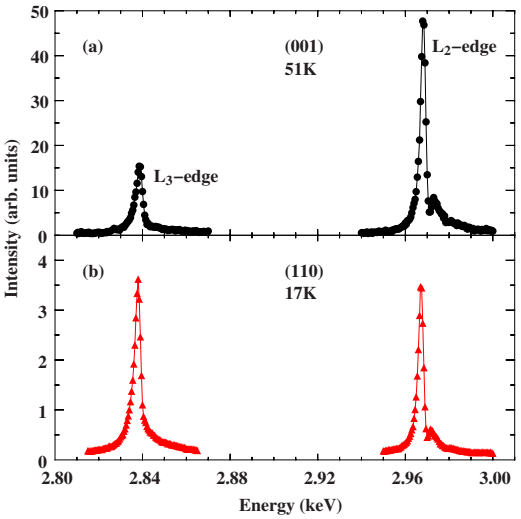

FIG. 2. (Color online) Energy dependence of the diffracted intensity at the magnetic reflections (001) and (110) near the *L*-absorption edges of Ru. The energy profiles are not corrected for absorption.

III. RESULTS AND DISCUSSION

A. Magnetic structure

The energy dependence of the scattered intensity at the magnetic reflections (001) and (110) is shown in Fig. 2. The intensities of both reflections show a strong resonant enhancement at the L_2- and L_3-absorption edges of Ru due to the electric dipole-allowed $2p\rightarrow4d$ transitions which directly probe the partially occupied 4*d* orbitals responsible for magnetism. The observation of a resonant signal at these positions agrees with *A*-type AFM order, as suggested by magnetization,[3] as well as Raman[8] and neutron scattering data.[13] Based on the absence of the (003) reflection in the neutron diffraction pattern, Yoshida *et al.*[13] proposed that the magnetic moments are aligned ferromagnetically within the bilayers and antiferromagnetically between adjacent bilayers. Our data are consistent with this suggestion since the (110) reflection would not be observed if another *A*-type AFM structure was realized.

In order to determine the direction of the magnetic moment, we studied the polarization and azimuthal-angle dependence of the intensity at (001) and (110). The experimental configuration is shown in Fig. 1. Here, σ and π denote the polarization components perpendicular and parallel to the diffraction plane, respectively. In the case of a horizontal scattering geometry, the incident beam has π-polarization and the total scattered intensity contains two polarization components, namely $\sigma'$and π'. α denotes the angle between the magnetic moment **m** and the scattering vector **Q**, and the azimuthal angle ψ describes the rotation of the sample about the scattering vector.

The azimuthal-angle dependence of the resonant signal at reflection (001) measured below and above T_{MI} is shown in Fig. 3(a). In the low temperature phase, the maximum intensity is observed when the *b*-axis lies in the scattering plane ($\psi=0°$), whereas the intensity almost vanishes when the *a*-axis is parallel to the diffraction plane ($\psi=90°$). The

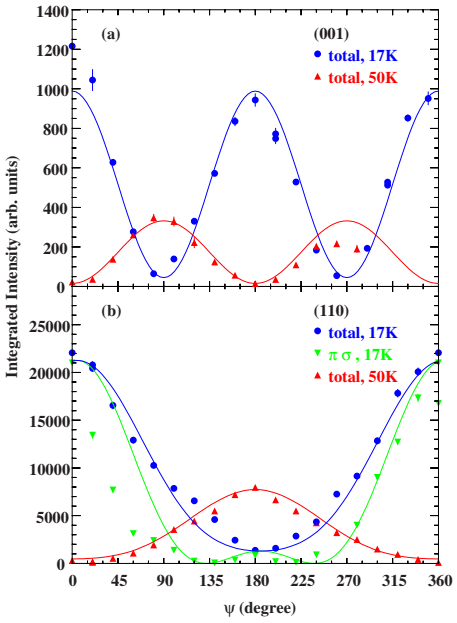

FIG. 3. (Color online) Azimuthal-angle dependence of the scattered intensity at the (001) and (110) reflection measured below and above T_{MI}. The solid lines are calculations based on the electric-dipole approximation and a magnetic moment direction along the b-axis below and along the a-axis above T_{MI}.

opposite behavior is found in the metallic AFM phase above T_{MI}, where the azimuthal dependence is shifted by 90° with respect to the one below T_{MI}. The azimuthal dependence of the scattered intensity at wave vector (110), as shown in Fig. 3(b), is quite different from that at (001). In the low temperature phase, the total intensity exhibits a maximum when the ab-plane coincides with the scattering plane, with the b-axis pointing toward the incident beam (ψ=0°). Above T_{MI}, the maximum intensity is found when the a-axis lies in the diffraction plane and points in the direction of the incident beam (ψ=180°).

The azimuthal dependences at both reflections suggest a magnetic moment direction along the b-axis in the low temperature phase and a reorientation to the a-axis at T_{MI}. We therefore calculated the azimuthal dependence of the scattered intensity for both reflections based on A-type AFM structures with these moment directions. Following the analysis described in Ref. 21, the intensity $I^{\mu\nu}$ in a particular polarization channel at (001) and (110) is given by

$$I^{\mu\nu} = \left| \sum_j e^{i\vec{Q}\vec{R}_j} g^{\mu\nu}_{\uparrow,\downarrow} \right|^2 \propto |g^{\mu\nu}_{\uparrow} - g^{\mu\nu}_{\downarrow}|^2, \tag{1}$$

where μ and ν denote the polarizations of the incident and diffracted beams, respectively, and $g_\uparrow$ and $g_\downarrow$ are the scattering lengths of the two spin directions, which are calculated as

$$g_\uparrow - g_\downarrow = \begin{pmatrix} g^{\sigma\sigma'}_{\uparrow} - g^{\sigma\sigma'}_{\downarrow} & g^{\pi\sigma'}_{\uparrow} - g^{\pi\sigma'}_{\downarrow} \\ g^{\sigma\pi'}_{\uparrow} - g^{\sigma\pi'}_{\downarrow} & g^{\pi\pi'}_{\uparrow} - g^{\pi\pi'}_{\downarrow} \end{pmatrix} = \begin{pmatrix} 0 & m_x \cos\theta + m_z \sin\theta \\ -m_x \cos\theta + m_z \sin\theta & -m_y \sin 2\theta \end{pmatrix}. \tag{2}$$

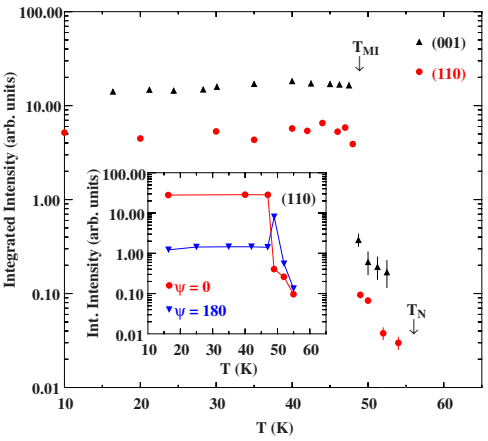

FIG. 4. (Color online) Temperature dependence of the integrated intensity at the magnetic reflections (001) and (110) taken at the azimuthal position ψ=0°. The inset shows the temperature dependence of the scattered intensity at wave vector (110) for ψ=0° and ψ=180°.

Here, θ is the scattering angle and $m_x = m \sin\alpha \cos\psi$, $m_y = m \sin\alpha \sin\psi$, and $m_z = -m \cos\alpha$ are the projections of the magnetic moment on the axes of the reference system. The calculated dependences, which are shown as solid curves in Fig. 3, are in good agreement with the experimental results, and hence, confirm magnetic moment orientations along the b-axis below and along the a-axis above T_{MI}.

The temperature dependence of the intensities of the two reflections is displayed in Fig. 4. Both reflections exhibit almost the same temperature dependence at ψ=0°, which corresponds to the maximum intensity position in the low temperature phase. Below T_{MI}, the intensity remains approximately constant with increasing temperature, followed by an intensity loss of approximately two orders of magnitude at T_{MI}. This drastic intensity change is mostly due to the reorientation of the magnetic moment and consistent with the azimuthal dependence in Fig. 3. In the metallic AFM phase, the intensity further decreases upon heating and continuously vanishes at T_N, as expected for a second-order phase transition. The inset of Fig. 4 shows the temperature dependence at the wave vector (110) for ψ=180°, where the moment reorientation results in an intensity enhancement by almost one order of magnitude above T_{MI}. From a comparison of the maximum intensities in the two phases, we conclude that the amplitude ratio of sublattice magnetizations in the metallic and insulating states is $\sim 1/\sqrt{3}$.

Antiferromagnetic metallic states such as the one observed in $Ca_3Ru_2O_7$ between T_N and T_{MI} are uncommon in oxides, but a related phenomenon has been observed in bilayer manganates which also exhibit A-type antiferromagnetism.[22] The small amplitude of the ordered magnetic moment in this phase is presumably a consequence of charge and/or orbital fluctuations. Below T_{MI}, a variety of experiments have provided indirect evidence of orbital order.[8,18,23] Because of the strong spin-orbit interaction and the relatively weak Jahn–Teller coupling of the $4d$ t_{2g} valence electrons, one generally expects an unquenched orbital magnetization in a state with ordered Ru orbitals. Additional terms in the spin Hamiltonian induced by the orbital moment

may then be responsible for the observed reorientation below T_{MI}.

B. Orbital order

In order to obtain direct evidence of orbital order, we searched for resonant superstructure reflections characteristic of a staggered ordering pattern ["antiferro-orbital order" (AFO)] at various high-symmetry positions in reciprocal space including (1/2 1/2 0), (1 0 0), (0 1 0), (1/2 0 0), and (0 1/2 0), with the photon energy tuned to one of the Ru L-absorption edges, but we did not find any signal above background. In Ca_2RuO_4, orbital order with the same propagation vector as the antiferromagnetically ordered state was inferred from the persistence of a weak resonant reflection above the magnetic ordering temperature.[12] An analogous phenomenon (namely, weak A-type AFO) would not be detectable in $Ca_3Ru_2O_7$ because the magnetic ordering temperature exceeds the onset of orbital order so that the magnetic intensity would dominate at all temperatures.

We also used a resonant diffraction method to check for the presence of a uniform polarization of the Ru orbitals ["ferro-orbital order" (FO)] in the insulating state. As FO manifests itself as resonant intensity at the main crystallographic Bragg reflections, it is difficult to separate this contribution from the regular Thomson scattering. To solve this problem, the authors of Refs. 24 and 25 developed an interference technique where the resonant FO signal is amplified by charge scattering. To this end, the analyzer is rotated out of the $\sigma\pi'$-position ($\phi_A=90°$), where the FO signal is expected to occur, to $\phi_A=90° \pm \Delta$ (see Fig. 1 for the definition of the angles). The scattered intensity at a rotational analyzer angle ϕ_A is given by

$$I(\phi_A) = |F_{\sigma\sigma'} \cos \phi_A - F_{\sigma\pi'} \sin \phi_A|^2 + |F_{\sigma\sigma'} \sin \phi_A + F_{\sigma\pi'} \cos \phi_A|^2 \cos^2 2\theta_A, \quad (3)$$

where $F_{\mu\nu}$ denote the form factors in the different polarization channels and θ_A is the scattering angle of the analyzer. This leads to the following interference term:

$$I(\phi_A = 90° - \Delta) - I(\phi_A = 90° + \Delta) \propto 2\,\mathrm{Re}(F_{\sigma\sigma'} F^*_{\sigma\pi'}) \sin^2 2\theta_A \sin^2 2\Delta. \quad (4)$$

In principle, this experiment can also be performed at the Ru L-edge where the FO signal is expected to be most pronounced. However, this option is unfavorable based on two considerations. First, all Bragg reflections that can be reached at this photon energy have a magnetic contribution that is expected to dominate the orbital one. Second, the polarization analyzer currently available for this energy, Si (111), has an extremely small mosaicity, which causes additional experimental problems. Following the protocol established in Refs. 24 and 25, we therefore performed the experiment at the K-absorption edge of Ru, using pyrolytic graphite as analyzer.

Figure 5 shows energy scans near the Ru K-absorption edge at the reflection (0 6 0) taken at two azimuthal positions. The difference of the two signals measured at ϕ_A $=85°$ and $\phi_A=95°$ does not indicate any FO contribution. In addition to the search for a FO signal within a wide azimuthal range of 180°, we also varied the angular difference Δ between the two analyzer positions, but no FO intensity was detected.

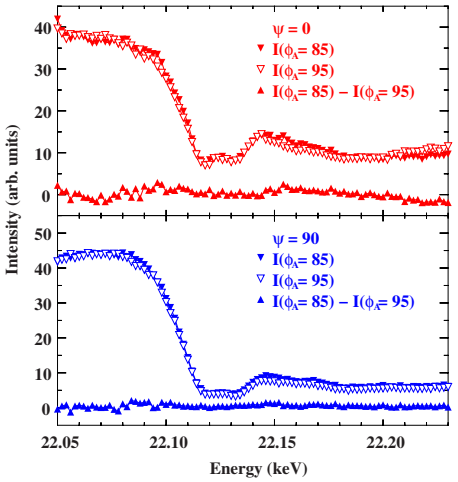

FIG. 5. (Color online) Energy scans for $\phi_A=85°$ and $\phi_A=95°$ at the reflection (060) taken at two azimuthal positions $\psi=0°$ and $\psi=90°$ measured at 20 K.

Since an experiment with a very similar design revealed a substantial FO signal for Ca_2RuO_4, we conclude that the amplitude of the FO order parameter, if present, is considerably weaker in $Ca_3Ru_2O_7$. This is not unexpected in view of the much lower metal-insulator transition temperature in $Ca_3Ru_2O_7$ and the apparent ability of a modest external magnetic field to rearrange or even obliterate the orbital order in this material.[15] Corresponding magnetic field-induced transitions have not been reported for Ca_2RuO_4. A reduction of the FO order parameter, yielding a resonant signal below our detection limit, could result from orbital quantum fluctuations and/or residual charge fluctuations in the insulating state.

IV. CONCLUSION

Resonant x-ray diffraction on a small single crystal has provided a comprehensive picture of the magnetic structure of $Ca_3Ru_2O_7$ in its insulating and metallic phases, illustrating the power of this method for magnetic structure determination in situations where large crystals for neutron diffraction are not available. As evidence for orbital order could not be found in $Ca_3Ru_2O_7$ within the experimental sensitivity, it is likely that the orbital-order parameter is substantially weaker than in its single-layer counterpart, Ca_2RuO_4. Weak orbital order, combined with strong spin-orbit coupling, are presumably at least partially responsible for the rich phase behavior of $Ca_3Ru_2O_7$ observed in response to external magnetic fields.

ACKNOWLEDGMENTS

We would like to thank F. Schaefers, M. Mertin, E. Dudzik, and R. Feyerherm for their assistance during beam

time at BESSY. Work at Cologne was supported by the DFG through SFB 608 and by the BMBF Project No. 05 ES3XBA/5. Work at Brookhaven was supported by the U.S. Department of Energy, Division of Materials Science, under Contract No. DE-AC02-98CH10886. Use of the Advanced Photon Source was supported by the U.S. Department of Energy, Office of Science, Office of Basic Energy Sciences, under Contract No. DE-AC02-06CH11357.

[1] A. P. Mackenzie and Y. Maeno, Rev. Mod. Phys. **75**, 657 (2003).
[2] R. A. Borzi, S. A. Grigera, J. Farrell, R. S. Perry, S. J. S. Lister, S. L. Lee, D. A. Tennant, Y. Maeno, and A. P. Mackenzie, Science **315**, 214 (2007).
[3] S. McCall, G. Cao, and J. E. Crow, Phys. Rev. B **67**, 094427 (2003).
[4] X. N. Lin, Z. X. Zhou, V. Durairaj, P. Schlottmann, and G. Cao, Phys. Rev. Lett. **95**, 017203 (2005).
[5] C. S. Nelson, H. Mo, B. Bohnenbuck, J. Strempfer, N. Kikugawa, S. I. Ikeda, and Y. Yoshida, Phys. Rev. B **75**, 212403 (2007).
[6] G. Cao, L. Balicas, Y. Xin, J. E. Crow, and C. S. Nelson, Phys. Rev. B **67**, 184405 (2003).
[7] C. S. Snow, S. L. Cooper, G. Cao, J. E. Crow, H. Fukazawa, S. Nakatsuji, and Y. Maeno, Phys. Rev. Lett. **89**, 226401 (2002).
[8] J. F. Karpus, C. S. Snow, R. Gupta, H. Barath, S. L. Cooper, and G. Cao, Phys. Rev. B **73**, 134407 (2006).
[9] G. Cao, K. Abbound, S. McCall, J. E. Crow, and R. P. Guertin, Phys. Rev. B **62**, 998 (2000).
[10] V. Varadarajan, S. Chikara, V. Durairaj, X. N. Lin, G. Cao, and J. W. Brill, Solid State Commun. **141**, 402 (2007).
[11] M. Kubota, Y. Murakami, M. Mizumaki, H. Ohsumi, N. Ikeda, S. Nakatsuji, H. Fukazawa, and Y. Maeno, Phys. Rev. Lett. **95**, 026401 (2005).
[12] I. Zegkinoglou, J. Strempfer, C. S. Nelson, J. P. Hill, J. Chakhalian, C. Bernhard, J. C. Lang, G. Srajer, H. Fukazawa, S. Nakatsuji, Y. Maeno, and B. Keimer, Phys. Rev. Lett. **95**, 136401 (2005).
[13] Y. Yoshida, S. I. Ikeda, H. Matsuhata, N. Shirakawa, C. H. Lee, and S. Katano, Phys. Rev. B **72**, 054412 (2005).
[14] G. Cao, S. McCall, J. E. Crow, and R. P. Guertin, Phys. Rev. Lett. **78**, 1751 (1997).
[15] G. Cao, X. N. Lin, L. Balicas, S. Chikara, J. E. Crow, and P. Schlottmann, New J. Phys. **6**, 159 (2004).
[16] Y. Yoshida, I. Nagai, S. I. Ikeda, N. Shirakawa, M. Kosaka, and N. Môri, Phys. Rev. B **69**, 220411(R) (2004).
[17] G. Cao, L. Balicas, Y. Xin, E. Dagotto, J. E. Crow, C. S. Nelson, and D. F. Agterberg, Phys. Rev. B **67**, 060406(R) (2003).
[18] J. F. Karpus, R. Gupta, H. Barath, S. L. Cooper, and G. Cao, Phys. Rev. Lett. **93**, 167205 (2004).
[19] F. Baumberger, N. J. C. Ingle, N. Kikugawa, M. A. Hossain, W. Meevasana, R. S. Perry, K. M. Shen, D. H. Lu, A. Damascelli, A. Rost, A. P. Mackenzie, Z. Hussain, and Z.-X. Shen, Phys. Rev. Lett. **96**, 107601 (2006).
[20] J. S. Lee, S. J. Moon, B. J. Yang, J. Yu, U. Schade, Y. Yoshida, S. I. Ikeda, and T. W. Noh, Phys. Rev. Lett. **98**, 097403 (2007).
[21] J. P. Hill and D. F. McMorrow, Acta Crystallogr., Sect. A **52**, 236 (1996).
[22] T. Kimura and Y. Tokura, Annu. Rev. Mater. Sci. **30**, 451 (2000).
[23] M. N. Iliev, S. Jandl, V. N. Popov, A. P. Litvinchuk, J. Cmaidalka, R. L. Meng, and J. Meen, Phys. Rev. B **71**, 214305 (2005).
[24] T. Kiyama, Y. Wakabayashi, H. Nakao, H. Ohsumi, Y. Murakami, M. Izumi, M. Kawasaki, and Y. Tokura, J. Phys. Soc. Jpn. **72**, 785 (2003).
[25] H. Ohsumi, Y. Murakami, T. Kiyama, H. Nakao, M. Kubota, Y. Wakabayashi, Y. Konishi, M. Izumi, M. Kawasaki, and Y. Tokura, J. Phys. Soc. Jpn. **72**, 1006 (2003).